Numerical Modeling of Ultrawideband Propagation Along a Wind Turbine Blade

Franek, Ondrej; Zhang, Shuai; Olesen, Kim; Eggers, Patrick Claus F.; Byskov, Claus; Pedersen, Gert F.

Published in:
I E E E Transactions on Antennas and Propagation

DOI (link to publication from Publisher):
10.1109/TAP.2018.2874489

Creative Commons License
Other

Publication date:
2018

Document Version
Accepted author manuscript, peer reviewed version

Numerical Modeling of Ultrawideband Propagation Along a Wind Turbine Blade

Ondřej Franek, *Member, IEEE*, Shuai Zhang, Kim Olesen, Patrick C. F. Eggers, *Member, IEEE*, Claus Byskov, and Gert F. Pedersen

***Abstract*—Full-wave numerical analysis of an ultrawideband wireless link in frequency band 3–5 GHz along a 37.3m long wind turbine blade is presented. The method used for the analysis is the well-established finite-difference time-domain (FDTD) method with staggered Yee mesh. Simulated results are compared to data obtained from measurement on a real blade, in two experiments involving antennas transmitting both from outside near the blade tip and from inside the blade. In the first experiment, when the wave is propagated along the entire blade and received near the blade root, the differences between the simulation and the measurement are found in pulse magnitudes within 3 dB and in delay within 1.5 ns. In the second experiment, the emitted waves are studied at only 10m distance, but at higher elevations, and the error reaches 6 dB in magnitude and 1.9 ns in delay. Possible reasons for observed discrepancies between the simulations and the measurements are briefly discussed. Despite the long distances involved and challenges connected to the numerical dispersion and anisotropy, the FDTD method turns out to be a feasible choice for full-wave numerical modeling of problems of this type, albeit with slightly high sensitivity to the underlying model.**

***Index Terms*—Ultrawideband antennas, Ultrawideband radiation, Microwave propagation, Dielectric bodies.**

I. Introduction

Wind energy is nowadays seen as one of the most important alternatives to fossil fuels in the world's endeavor for sustainability and reducing carbon dioxide emissions [1]. To reduce the unit cost of electricity, each new generation of wind turbines is being equipped with longer blades than its predecessor, since longer blades can harvest energy from larger area of the wind field [2]. At the same time, the blades are being made of lighter composite materials to avoid increased loads on the supporting structures, ie. the tower and the nacelle. However, all wind turbine blades change their shapes and bend towards the tower under strong wind loads, and this effect is more pronounced with longer and lighter blades. This in turn leads to the necessity of shutting down turbines with large rotors even under moderately strong winds, otherwise the risk of catastrophic collision of the blades with the tower would be too high [3]. If the actual deflection of the blade was known in real time, the turbine controls could adaptively pitch individual blades out of the wind load and prevent the tower strike while maintaining regular operation. The result would be more energy harvested as the turbine would be able to safely operate even under stronger winds.

In our previous papers, we have introduced a wind turbine blade deflection sensing system [4] based on ultrawideband (UWB) radio technology [5]. The system consists of one antenna mounted at the tip and two antennas mounted at the root of a blade, and the blade deflection is determined by timing the traversal of a signal with pulsed waveform between the tip and the root. With the help of measurements on a real wind turbine blade it has been demonstrated that such system is feasible. However, it also became clear that the positions of the antennas at the root will need to be optimized in order to guarantee sufficient link budget and pulse clarity, and that this will need deeper understanding of the propagation effects along the blade. Since the blade has a highly irregular shape, it is not possible to estimate the link properties using asymptotic formulas, numerical analysis of the problem is needed instead.

Propagation on long distances is typically solved using ray based techniques [6], [7]. These are not suitable for the problem at hand, however, because the surface grazing mode of propagation and proximity of the tip antenna to the blade structures give rise to surface traveling wave and near field effects that cannot be modeled by ray tracing. The near field effects could alternatively be modeled by integral equation methods such as the method of moments (MoM) [8] or the multilevel fast multipole method (MLFMA) [9], but the combination of large size of the blade, its elongated hollow shape (many surfaces), dielectric material and wide frequency band makes the problem challenging even for MLFMA. For this study, the finite-difference time-domain (FDTD) method [10] has been chosen instead. Of the full-wave methods capable of accurately modeling near-field phenomena, FDTD method seems to be the most efficient and naturally fitting to analysis of UWB propagation thanks to its time domain formulation. On the other hand, FDTD still requires quite large computational resources when it comes to structures several wavelengths long such as the wind turbine blade, aircraft or ships [11]–[14].

To be able to perform the simulations on a personal computer, some initial investigations into the propagation characteristics of the system have been made using a relatively short 4.5m long section of the blade near the tip antenna [15]. Another numerical analysis using blade section with length 2.5 m revealed some interesting phenomena regarding the leaky waves traveling along the blade surface [16], which confirmed the generally complicated character of wave propagation along dielectric waveguides [17]. The results also offered valuable

O. Franek, S. Zhang, K. Olesen, P. C. F. Eggers, and G. F. Pedersen are with the Antennas, Propagation and Millimetre Wave Systems section, Department of Electronic Systems, Aalborg University, DK-9220 Aalborg Øst, Denmark (e-mail: of@es.aau.dk)

C. Byskov is with LM Wind Power, DK-6000 Kolding, Denmark

Manuscript received January 31, 2018. This work was supported by the Innovation Fund Denmark (iRotor project).

insight into required positions of the root antennas, but it could not provide us with quantitative estimates for the link budget or with information about UWB pulse distortion after traveling the whole blade length.

In this paper, we present results of numerical analysis of the full UWB wireless link at frequency band 3–5 GHz between the tip and the root antennas, ie. along almost the entire 37.3 m long wind turbine blade, using the FDTD method. The simulations are compared to measurements performed using vector network analyzer (VNA) and two types of antennas on a real blade. It is shown that in this experiment the pulse arrival times are predicted by the FDTD method within 1.5 ns and that the link budget can be estimated with accuracy of 3 dB. A second experiment with shorter distances between the antennas but higher elevations with respect to the blade surface showed increased magnitude errors up to 6 dB, and delay errors up to 1.9 ns. Even though the results seem to be very sensitive with respect to the dielectric properties of the blade material and possibly also the shape of the blade, the FDTD method proved to be a viable way to model propagation in scenarios when the signal path is running parallel or almost parallel to dielectric objects.

Overall, this paper demonstrates that UWB propagation along large dielectric structures with complex-shaped profiles, such as the wind turbine blade analyzed here, can be successfully modeled by the FDTD method, even though it is necessary to take into account certain sources of errors and sensitivity to the underlying model. These findings may prove useful to all readers who at some point would need to analyze UWB propagation either along wind turbine blades or objects of similar shape and material, such as helicopter rotor blades, fiberglass aircraft fuselages, or ship hulls. Contributions on large-scale simulations in the available literature [11]–[14] present purely metallic objects, lack detailed information on the pulses propagated along the body, and do not compare the results against measurements. To our best knowledge, full-wave numerical analysis of radio propagation along a wind turbine blade, or any other elongated object with similar shape and dielectric material, including comparison to measurements has not yet appeared in the available literature.

The paper is organized as follows. In Section II, the principle of the UWB blade deflection sensing system is briefly explained. Section III contains description of the simulation technique and the numerical model of the blade used in the simulations. In Section IV, the first experiment with propagation along the entire 37.3m-long blade is described, and the measured and the simulated results are presented and discussed. In Section V, the second experiment that consisted of measuring the field profiles with increasing height over the blade at 10m distance is presented, together with the measurement and simulation results. Finally, conclusions are offered in Section VI.

II. Deflection Sensing System

The deflection sensing system has been described in detail in [4], here we repeat the main features only. The system consists of a transmitting (TX) antenna placed at the tip of the blade and two receiving (RX) antennas positioned near the blade root (Fig. 1). The deflection of the blade is determined by detecting the time of arrival of UWB pulses with frequency range 3–5 GHz launched from the tip antenna.

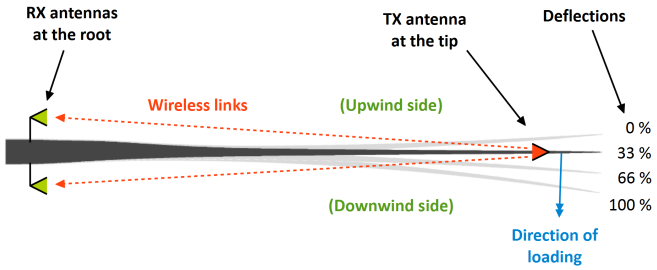

Fig. 1. Principle of the blade deflection sensing system

Due to the clearance between the blade root and the tower, the root antennas cannot be mounted more than approx. 1.5 m from the blade surface. Similarly, the tip antenna must be placed very close to the blade surface, or ideally inside it, so that it does not produce excessive aerodynamic noise and reduce the efficiency of the blade. It is clear that with this arrangement it is basically impossible to keep line-of-sight conditions between the tip and the root antennas at all times, because the blade bends in both directions, downwind (towards the tower) as well as upwind (away from the tower). Having two antennas at the root helps to increase the likelihood of relatively unobstructed path and, as a result, increases the robustness of the system, but the vicinity of the fiberglass body to the wireless link still causes multipath effects.

It should be noted, however, that not all multipath components in the received signal necessarily pose a problem. Those components that arrive at the root antenna relatively late are harmless because the intended pulse detector, which is an improved correlation estimator [18], locks only on the rising edge of the first received pulse. It is only when the secondary path of the signal has similar length as the primary (direct) signal that the main body of the pulse can be distorted. Preventing the distortion of the received pulse is the main challenge of the design.

III. FDTD Simulation Description

The simulation method was the 2^{nd} order 3D Yee-FDTD method [10] implemented in our in-house numerical code. The simulation could of course be performed by any of the commercially available electromagnetic solvers, but we have chosen our in-house FDTD code due to its CPU and memory efficiency when dealing with large models such as the wind turbine blade analyzed in this work. The frequency range of the Gauss-sine excitation pulse was 3–5 GHz, and as a consequence the mesh cell size was chosen 5 mm. This choice resulted in resolution of 12 cells per wavelength at the highest frequency in free space, but substantially less inside the fiberglass material. The entire computational domain dimensions were 1279 $\times$ 1277 $\times$ 7531 cells, which totals to 12.3 billion mesh cells. The perfectly matched layer (PML) absorbing boundary condition is included in this number. As the shape of the domain is elongated and the waves are

supposed to travel along the highest dimension, the thickness of the PML layer needed to be 50 cells, in order to prevent spurious reflections at low incidence angles. One simulation of the entire blade took approx. 17 hours to finish on our 288-core cluster.

Due to long running times, the RX antennas were not included in the simulations as a full model, because that would require running a new simulation on every change in position of the RX antenna, impeding optimization of the position. To speed up the process, only the E-field vector components at the desired positions of the RX antennas were recorded and the true output signal was reconstructed by multiplying (in frequency domain) the E-fields with effective lengths of the actual RX antennas. On the other hand, the TX antenna was included as a full model, as there were not that many positions over which they were iterated, besides the fact that replacing the tip antenna positioned very close or inside the blade by its effective length would violate the far-field condition under which the effective length is defined.

The 37.3 m long wind turbine blade was represented by a realistic voxel model with resolution 5 mm, the same as the discretization step of the FDTD method. The properties of the blade material have been obtained by measurement of a fiberglass sample using the SPEAG DAK-TL system with DAK3.5-TL probe [19], giving $\varepsilon = 3$ and $\tan\delta = 0.01$ at 4 GHz. Corresponding resolution was slightly below 7 cells per wavelength at the highest frequency, which is below the recommended 10-cell limit, raising concerns about excessive numerical dispersion error of the simulation [10]. However, a test simulation run on a short segment of the blade with double resolution (2.5 mm cell size) showed no significant improvement over the original resolution (5 mm), so we could safely conclude that the received pulse is not influenced by the short wavelength in the fiberglass.

On the other hand, the dispersion error was significant when observing pulses traveling along the full path from the tip to the root antennas, almost the entire length of the blade. The distance between the antennas on the blade is approx. 33 m, which is 330 free-space wavelengths at 3 GHz and 550 free-space wavelengths at 5 GHz. Assuming the phase error of FDTD operating in 10 cells per wavelength regime is approx. 1 degree per wavelength, there was considerable dispersion present and the received pulses were severely distorted. To mitigate this problem, we employed a dispersion compensation technique in the postprocessing of the results [20], [21].

IV. Experiment 1: Dynamic Pull Test

In this experiment, the 37.3m-long blade was mounted horizontally on a test stand with its leading edge pointing upwards and it was bent in the downwind direction using a pulling clamp attached to the tip (Fig. 2). Each wind turbine blade is manufactured with a certain prebend, ie. bending in the upwind direction, and the initial position of the pull test denoted as 0 % corresponded to this shape. During the pull test, the blade was continuously deflected in the downwind direction with stops at 33, 66 and eventually 100 % of the maximum pull, and then slowly released back to 0 % (prebend).

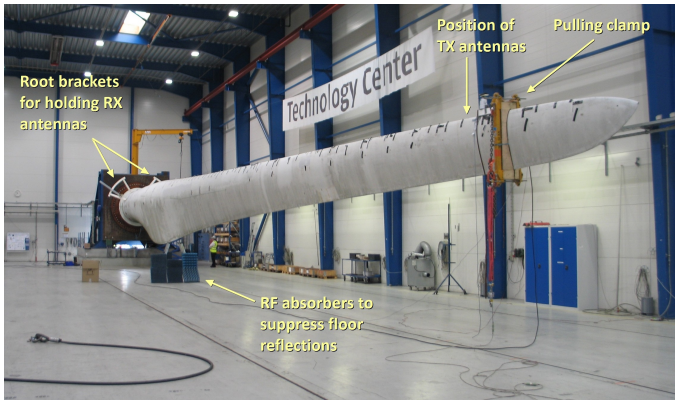

Fig. 2. Setup of Experiment 1 – the dynamic pull test. The blade can be seen from its downwind side. The cable that will be attached to the pulling clamp and perform the bending is visible lying on the floor, bottom left.

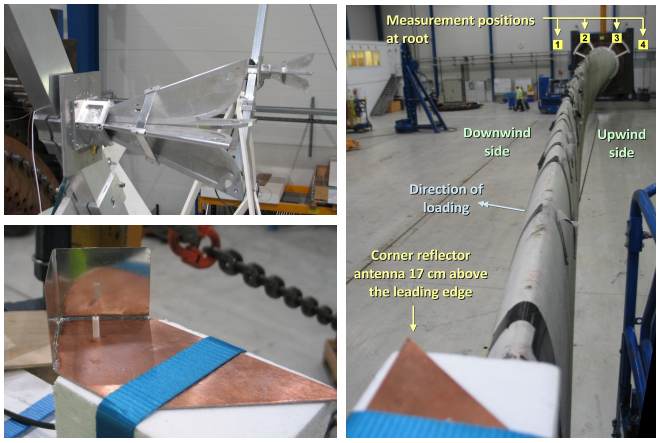

Fig. 3. Top left: Dual-polarized quad-ridged horn antennas used as the RX antennas at the root; Bottom left: Corner reflector antenna used as the TX antenna at the blade tip; Right: View from the tip towards the root when the blade is the prebend state. Positions of the RX antennas at the root are denoted. The corner reflector antenna sitting on a 17 cm high styrofoam block can partially be seen in the front.

The root antennas were mounted on brackets attached to the blade at the distance of 1.5 m from the mounting flange where the blade root ends. The attachment points can be seen in Fig. 3. The positions were selected to have various heights over the blade surface and angles from vertical, but always in symmetrical pairs in downwind and upwind directions. The antennas were dual-polarized quad-ridged horns covering frequency range from 700 MHz to 6 GHz with gain approximately 10 dBi [22].

The tip antenna was a monopole on a ground plane equipped with corner reflector (Fig. 3), which covered the 3–5 GHz band with gain approx. 9 dBi. This antenna was successively placed in two different positions. First, it was mounted at a styrofoam support 17 cm above the leading edge of the blade, with its phase center (monopole) positioned at the distance 34.56 m from the root flange. Second position of the tip antenna was inside the blade, in the hollow compartment approx. 25 cm below the blade leading edge, with the phase center 34.06 m from the root flange, ie. 0.5 m closer to the root than in the previous outside position. In both positions, the tip antenna

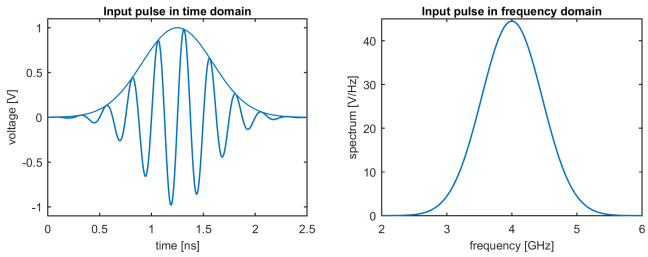

Fig. 4. Gauss-sine pulse serving as the input pulse in both simulations and measurements, in time domain (left) and in frequency domain (right).

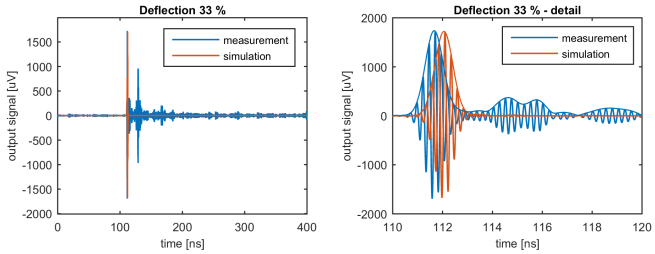

Fig. 5. Example of the signals at the RX output, for RX position 3 (upwind side) and 33 % deflection; full range (left) and detail with envelopes (right).

was vertically polarized, with its ground plane at the bottom and its beam pointing slightly upwards from the direction aimed at the root.

The measurements of the wireless link between the antennas were carried out with Keysight N5231A microwave network analyzer [23] in frequency sweep regime. Back-to-back calibration was done at the input connectors of the antennas. The output pulse waveforms at the root antennas were obtained in postprocessing, by multiplying the s_{21} with the Gauss-modulated sine pulse with frequency range 3–5 GHz (see Fig. 4) in frequency domain and then transforming into time domain. The pulses shown in this paper are thus the time domain responses of the entire wireless chain including the antennas to the excitation by the pulse in Fig. 4. An example of full shape of the output pulse waveforms is shown in Fig. 5. For easier reading of the plots, only envelopes of the signals are displayed in the following figures.

In Figs. 6 and 7 the output signals under different deflections of the blade are shown for root antenna positions 2 and 3, respectively, when the tip antenna is outside the blade. The simulated output pulse is added to the plot for deflection 33 %, because that one corresponds to the blade having straight shape, just like the numerical model used for the simulations. Figs. 8 and 9 show details of the pulsed waveforms in Figs. 6 and 7, respectively, in linear scale. The numerically predicted pulse has correct shape, very good agreement in magnitude and the delay error is within 0.4 ns which corresponds to 12 cm overshoot in free space. This error could be explained by the RX antennas being mounted on fixtures in front of the brackets, thus being positioned several centimeters closer to the TX antenna.

Magnitudes of the signal peaks and their delays for the outside position of the tip antenna are summarized in Fig. 10. The signal peak values were determined heuristically, identifying

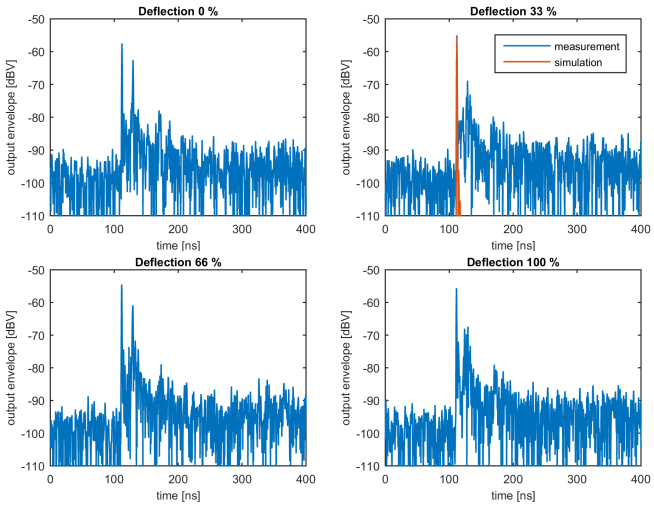

Fig. 6. Signal envelope at the RX antenna output when the TX antenna is mounted outside the blade 17cm above the leading edge, for four different deflections of the blade; RX position 2 (downwind side).

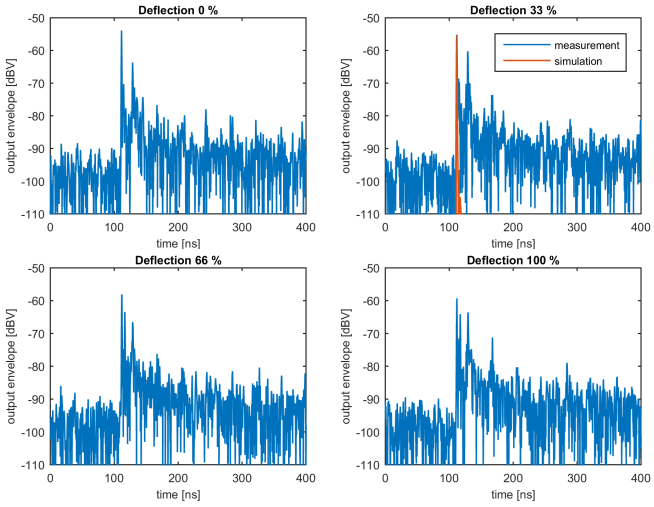

Fig. 7. Signal envelope at the RX antenna output when the TX antenna is mounted outside the blade 17cm above the leading edge, for four different deflections of the blade; RX position 3 (upwind side).

the first dominant peak in the data, and then reading its level and delay at the maximum. It can be seen how the magnitude slightly grows and delay shrinks at position 2 (to the left as seen from the tip) when the blade is deflected from upwind (prebend) deflection towards downwind (also to the left as seen from the tip). This behavior makes sense physically, since with stronger downwind deflection the tip is closer to the left side, causing shorter delay of the pulse, and the propagation path is less obstructed by the blade, resulting in stronger pulses. The tendency for position 3 (to the right as seen from the tip) is exactly opposite, as expected.

The next set of figures shows the measured and simulated data in the situation when the tip antenna is placed inside the blade, approx. 25 cm below the leading edge. Figs. 11 and 12 show the entire output signals in dB scale, and Figs. 13 and 14 the corresponding details in linear scale, for root antenna positions 1 and 4, respectively. The peak magnitudes

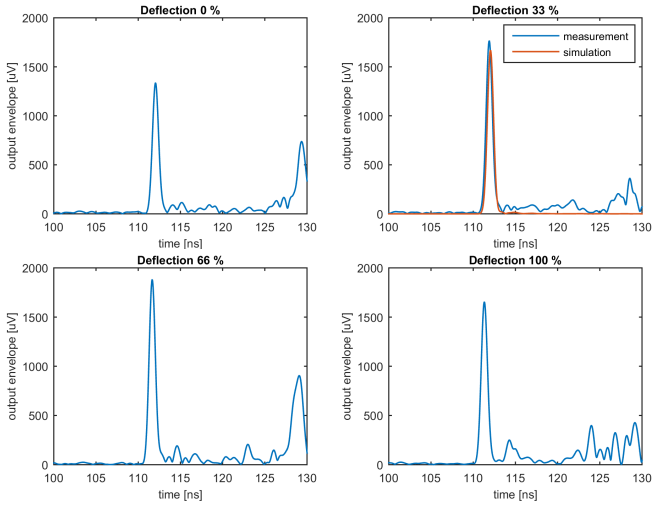

Fig. 8. Linearly scaled detail of signal envelope at the RX antenna output when the TX antenna is mounted outside the blade 17cm above the leading edge, for four different deflections of the blade; RX position 2 (downwind side).

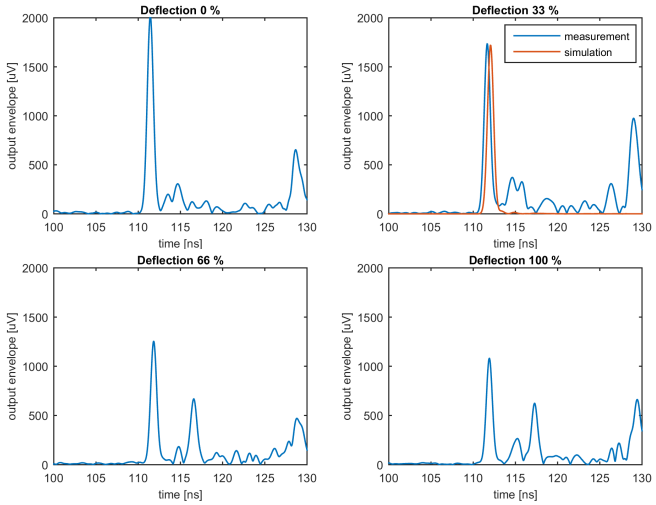

Fig. 9. Linearly scaled detail of signal envelope at the RX antenna output when the TX antenna is mounted outside the blade 17cm above the leading edge, for four different deflections of the blade; RX position 3 (upwind side).

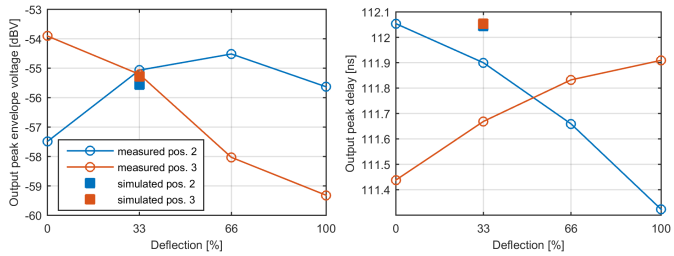

Fig. 10. Output signal envelope peaks (left) and peak delays (right) when the TX antenna is mounted outside the blade 17cm above the leading edge.

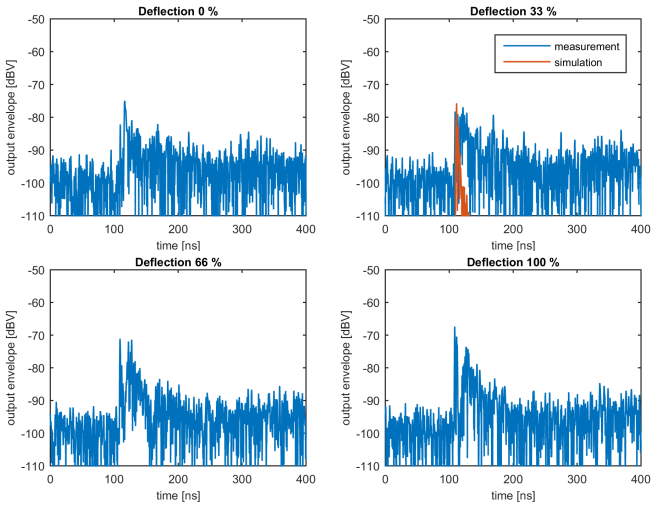

Fig. 11. Signal envelope at the RX antenna output when the TX antenna is mounted inside the blade 25cm below the leading edge, for four different deflections of the blade; RX position 1 (downwind side).

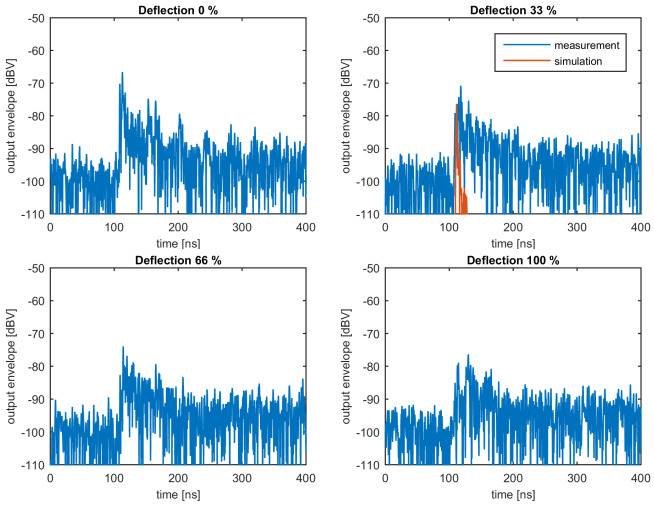

Fig. 12. Signal envelope at the RX antenna output when the TX antenna is mounted inside the blade 25cm below the leading edge, for four different deflections of the blade; RX position 4 (upwind side).

and delays are then summarized in Fig. 15, where the relevant peaks were again identified heuristically. If the signal levels are low, the uncertainty of the peak identification is naturally higher, such as in the case of RX position 4 and 100 % deflection (bottom right plot in Fig. 14). In this particular case, the pulse detector of the actual deflection sensing system would most likely fail, which is also why the system requires two RX antennas for successful operation, one at the upwind side and one at the downwind side of the blade.

The agreement in magnitude is within 3 dB, however the simulated pulses show considerable multipath distortion not present in the measurement, and they are also delayed considerably behind the measured. Please note that the direct path pulses in Figs. 13 and 14 are those with much smaller magnitude and earlier arrival than the multipath components. Possible explanation for the discrepancy is that the 33 % deflection of the blade at which the propagation has been

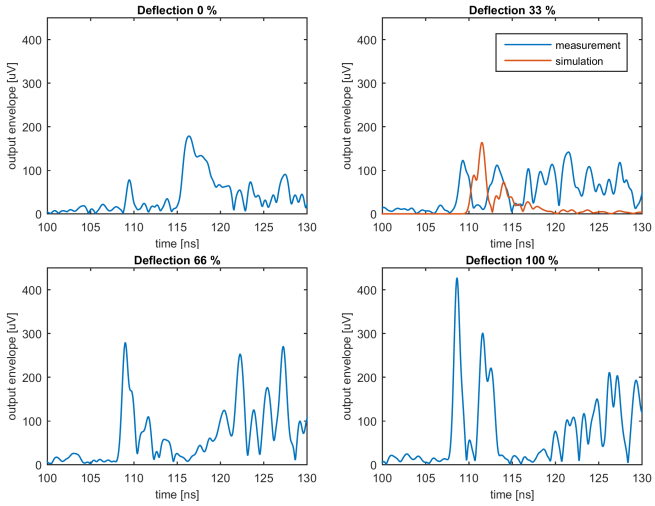

Fig. 13. Linearly scaled detail of signal envelope at the RX antenna output when the TX antenna is mounted inside the blade 25cm below the leading edge, for four different deflections of the blade; RX position 1 (downwind side).

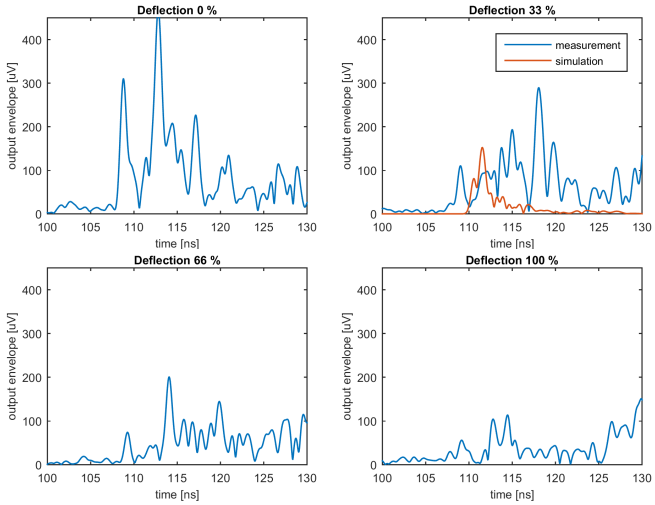

Fig. 14. Linearly scaled detail of signal envelope at the RX antenna output when the TX antenna is mounted inside the blade 25cm below the leading edge, for four different deflections of the blade; RX position 4 (upwind side).

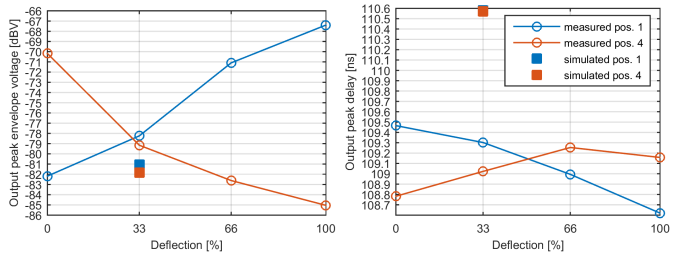

Fig. 15. Output signal envelope peaks (left) and peak delays (right) when the TX antenna is mounted inside the blade 25cm below the leading edge.

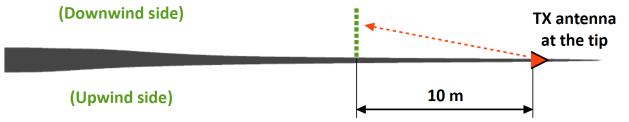

Fig. 16. Schematic of experiment 2: 37.3m long blade mounted in straight shape (without prebend) and with downwind side facing up. The signal was measured on a vertical line with height varying from 30 to 1200 mm above the surface (denoted by green dots).

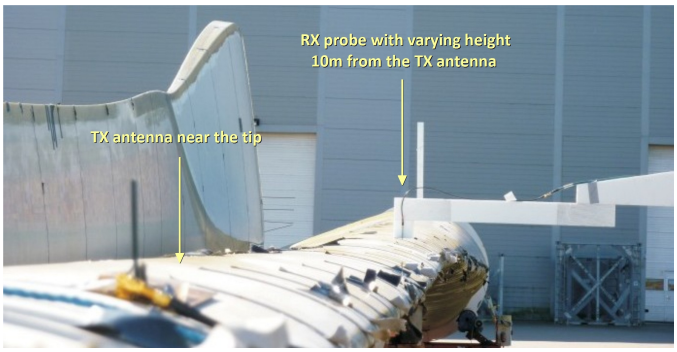

Fig. 17. Setup for experiment 2: 37.3m long blade with downwind side facing up. The TX antenna (OnGround type) is in the front, while the measurement arm with the RX probe is 10 m away.

measured does not entirely correspond to the shape of the blade that was numerically modeled. Another reason for different multipath effects may be differences in the fiberglass material properties between the measured blade and the sample from which the values used in the simulations were obtained. Either way, the outcome of the comparison is that longitudinal propagation of UWB pulses strongly interacting with the blade structure is considerably sensitive to the parameters of the blade numerical model.

V. Experiment 2: Height Profile

Another experiment we made was to find out the height profiles of the fields emitted from the tip antenna at the distance of 10 meters. This was done to determine if and how the radiation pattern of the tip antenna affects radiation from the blade. The distance between the TX and RX positions was reduced to 10 m to achieve better robustness in the results and avoid the "humps" of the blade near the root. A sketch of the experimental setup is displayed in Fig. 16. The fields were measured on a vertical line at heights spanning from 30 mm (the smallest possible distance of the RX probe phase center from the surface) to 1230 mm above the blade surface, aligned with the center of the root. A special positioning arm was constructed for this experiment, made of styrofoam (partially visible in Fig. 17) to minimize its impact upon the measurement.

The TX antennas at the tip were of two types. The first type was a ground-mounted dielectric-enhanced aperture with three directors ("OnGround" in further text) with gain approx. 12 dBi and main beam tilted upwards approx. 20 degrees (Fig. 18) whereas the second one was a corrugated Vivaldi aperture (denoted "Vivaldi") with gain of 10 dBi (Fig. 19). Both antennas covered the entire frequency range of the

Fig. 18. Three arrangements of the TX antenna: OnGround antenna outside (top), OnGround antenna inside (bottom left) and Vivaldi antenna inside (bottom right).

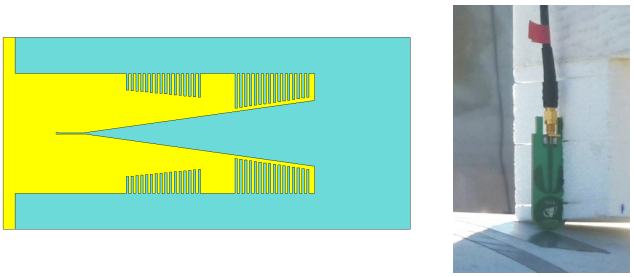

Fig. 19. The corrugated Vivaldi antenna used as a TX antenna (left) and the UWB dipole used as an RX probe (right).

measurement (3–5 GHz) and were placed so that they emitted vertical polarization, ie. perpendicular to the blade surface (cf. Fig. 17). Three different arrangements were tested, as shown in Fig. 18: a. OnGround antenna outside of the blade sitting on the surface 10 cm from the leading edge, b. OnGround antenna placed inside the blade, in the compartment between the blade web and its leading edge, and c. Vivaldi antenna also placed inside the blade.

The RX probe was a vertically oriented UWB dipole with gain of approx. 3 dBi attached to the styrofoam positioning arm (Fig. 19). The measurement equipment and processing was the same as in the previous experiment, see Sec. IV.

The height profiles of the output signal envelope peaks in the three aforementioned tip antenna arrangements are displayed in Fig. 20. Due to the presence of multipath components in the received signal, the output peaks appearing later than 37.5 ns were ignored for this purpose. It can be seen that, analogously to the previous experiment, the FDTD simulation predicts well the outcome when the TX antenna is outside, with errors within 3 dB, but once the TX antenna is placed inside the blade

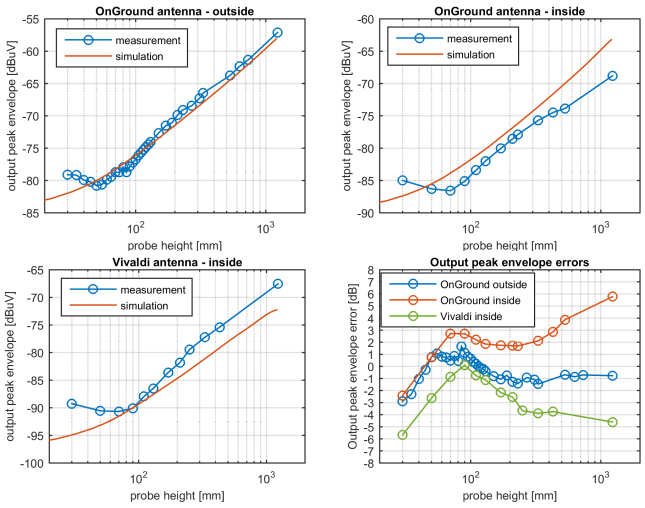

Fig. 20. Signal envelope peaks at the RX probe output when the OnGround antenna is mounted outside the blade 10cm from the leading edge (top left); OnGround antenna is mounted inside the blade next to the web (top right); Vivaldi antenna is mounted inside the blade next to the web (bottom left); Comparison of the envelope errors for the three TX antenna arrangements (bottom right).

higher discrepancies occur, up to 6 dB. It should be noted, however, that the comparison is apparently not very reliable for too low heights over the surface, where the measurement shows elevated values not present in the simulations. Here, the measured data is most likely affected by the proximity of the blade surface, causing detuning of the antenna.

The delays of the pulses are shown in Fig. 21. If we disregard the lower end of the height range, up to approx. 50 mm (20 mm from the edge of the dipole), where the measured fields may be spoiled by the detuning, the delay error does not exceed 1.5 ns, otherwise it can reach 1.9 ns for the two TX antennas placed inside. It is important to point out that a consistent bias can be seen in the delays. The measured signals are all delayed by at least 0.7 ns, corresponding to distance of 21 cm in air, which may be a result of an extra length of a short piece of cable unaccounted for in the back-to-back calibration measurements. It is assumed that the 1230 mm height point, where this bias is lower in all three instances, is affected by some other kind of error, maybe related to the scanning arm.

The output signal envelopes for the three TX antenna arrangements can be seen in detail in Figs. 22, 23 and 24, for four different heights above the surface. The multipath components are prominent, in particular there is one peak appearing consistently around 38.5 ns, which is suspected to be a reflection from the ground or another blade parked nearby (can be seen in Fig. 17 on the left).

In general, it can be said that the pulse modeling by the FDTD method is good as long as the TX antenna is outside and the radio waves do not need to penetrate the blade shell. The results for the inside placement of the TX antennas are less satisfying. Again, these differences may be attributed to mismatch between the simulated and the actual shape of the blade (model fidelity) and possible mismatch in material parameters.

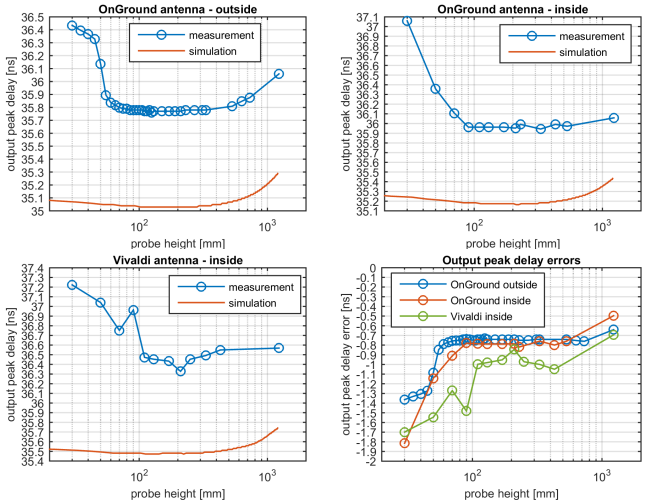

Fig. 21. Signal envelope peak delays at the RX probe output when the OnGround antenna is mounted outside the blade 10cm from the leading edge (top left); OnGround antenna is mounted inside the blade next to the web (top right); Vivaldi antenna is mounted inside the blade next to the web (bottom left); Comparison of the delay errors for the three TX antenna arrangements (bottom right).

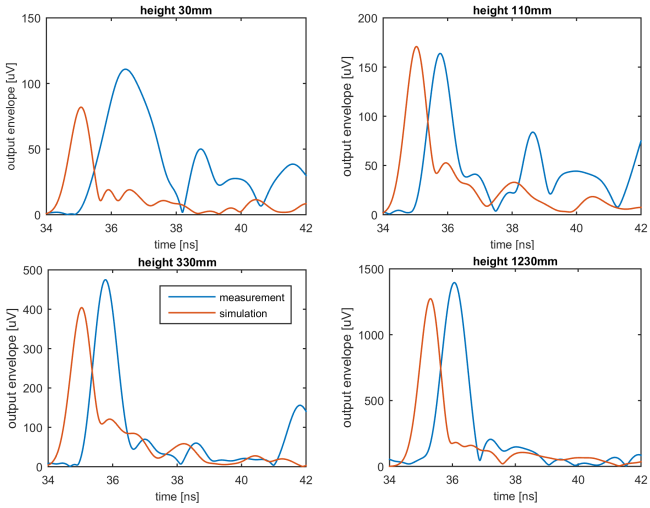

Fig. 22. Signal envelope at the RX probe output when the OnGround antenna is mounted outside the blade 10cm from the leading edge; four different heights of the RX probe.

VI. Conclusion

In this paper, we have presented description and results of numerical modeling of a UWB wireless link on a 37.3m long wind turbine blade using the FDTD method. The results were compared to data obtained from measurement on a real wind turbine blade of the same type as simulated. It has been found that when the tip antenna is placed outside the blade, and so the entire wireless link runs through air only, the agreement between the simulated and measured magnitudes and delays is very good. When the tip antenna is embedded inside the blade and the signal needs to penetrate the shell to reach the other end, the match is less satisfactory. In the first experiment, with the UWB signal traversing the entire length of the blade, the envelope magnitudes of simulation

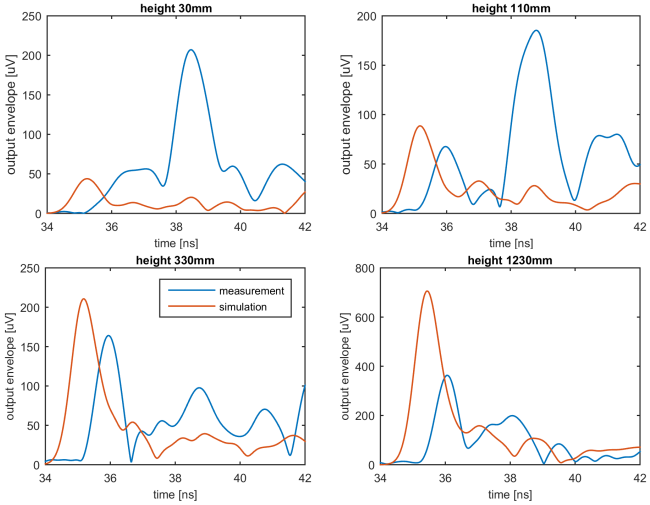

Fig. 23. Signal envelope at the RX probe output when the OnGround antenna is mounted inside the blade next to the web; four different heights of the RX probe.

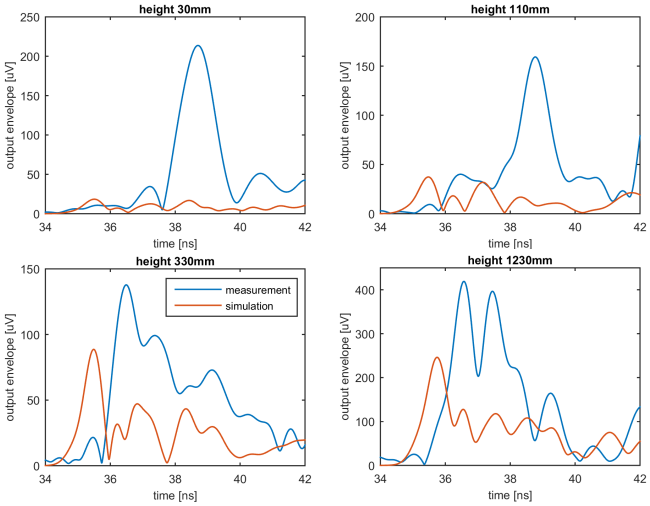

Fig. 24. Signal envelope at the RX probe output when the Vivaldi antenna is mounted inside the blade next to the web; four different heights of the RX probe.

and measurement were within 3 dB and the delay error within 1.5 ns, with some differences between the pulse shapes. The second presented experiment, height profiles at 10m distance, had the magnitudes differ by up to 6 dB and the delays up to 1.9 ns. We speculate that the differences may be attributed to possible mismatch between the actual shape of the blade and its numerical model, as well as mismatch between the corresponding material properties.

It can be concluded that using the FDTD method for propagation studies, even for several hundred wavelength long wireless links, is practical and viable, but on interaction with dielectric objects under high angles the method seems very sensitive to the underlying model. In our future work, we would like to demonstrate numerical modeling of even longer blades, over 50 meters long, and made of carbon fiber composites.

REFERENCES

[1] K. Grogg, "Harvesting the wind: the physics of wind turbines," *Physics and Astronomy Comps Papers*, p. 7, 2005.

[2] D. E. Berg, "Wind energy conversion," in *Handbook of energy efficiency and renewable energy*, F. Kreith and D. Y. Goswami, Eds. CRC Press, 2007, ch. 22, pp. 1–30.

[3] D. Ying, X. Ting, Z. Guoqiang, L. Hang, and T. De, "Blade tip deflection calculations and safety analysis of wind turbine," in *2nd IET Renewable Power Generation Conference (RPG 2013)*. IET, 2013, pp. 1–5.

[4] S. Zhang, T. L. Jensen, O. Franek, P. C. Eggers, K. Olesen, C. Byskov, and G. F. Pedersen, "UWB wind turbine blade deflection sensing for wind energy cost reduction," *Sensors*, vol. 15, no. 8, pp. 19 768–19 782, 2015.

[5] J. H. Reed, *An introduction to ultra wideband communication systems*. Prentice Hall PTR, 2005.

[6] R. Vaughan and J. B. Andersen, *Channels, Propagation and Antennas for Mobile Communications*. London: IEE, 2003.

[7] Z. Yun and M. F. Iskander, "Ray tracing for radio propagation modeling: Principles and applications," *IEEE Access*, vol. 3, pp. 1089–1100, 2015.

[8] R. F. Harrington, *Field computation by moment methods*. Wiley-IEEE Press, 1993.

[9] J. Song, C.-C. Lu, and W. C. Chew, "Multilevel fast multipole algorithm for electromagnetic scattering by large complex objects," *IEEE Trans. Antennas Propag.*, vol. 45, no. 10, pp. 1488–1493, 1997.

[10] A. Taflove and S. C. Hagness, *Computational electrodynamics: The Finite-Difference Time-Domain Method*, 3rd ed. Boston: Artech House, 2005.

[11] M. Kunze, Z. Reznicek, I. Munteanu, P. Tobola, and F. Wolfheimer, "Solving large multi-scale problems in CST STUDIO SUITE an aircraft application," in *2011 International Conference on Electromagnetics in Advanced Applications (ICEAA)*. IEEE, 2011, pp. 110–113.

[12] G. Cakir, M. Cakir, and L. Sevgi, "An FDTD-based parallel virtual tool for RCS calculations of complex targets," *IEEE Antennas Propag. Mag.*, vol. 56, no. 5, pp. 74–90, 2014.

[13] H. Li, H. Zhou, Y. Liu, X. Bao, and Z. Zhao, "Massively parallel FDTD program JEMS-FDTD and its applications in platform coupling simulation," in *2014 International Symposium on Electromagnetic Compatibility (EMC Europe)*. IEEE, 2014, pp. 229–233.

[14] S. Futatsumori, K. Morioka, A. Kohmura, N. Yonemoto, T. Hikage, K. Yahagi, M. Shirafune, M. Yamamoto, T. Nojima, and S. Narahashi, "Aircraft electromagnetic field estimation for wireless avionics intra-communication band using large-scale FDTD analysis–field estimation of A320 class passenger aircraft at 4 GHz band," in *2017 International Applied Computational Electromagnetics Society Symposium—Italy (ACES)*. IEEE, 2017, pp. 1–2.

[15] S. Zhang, T. L. Jensen, O. Franek, P. C. Eggers, C. Byskov, and G. F. Pedersen, "Investigation of a UWB wind turbine blade deflection sensing system with a tip antenna inside a blade," *IEEE Sensors J.*, vol. 16, no. 22, pp. 7892–7902, 2016.

[16] S. Zhang, O. Franek, P. C. Eggers, C. Byskov, and G. F. Pedersen, "Multipath suppression with an absorber for UWB wind turbine blade deflection sensing systems," *IEEE Trans. Microw. Theory Tech.*, vol. 65, no. 7, pp. 2583–2595, 2017.

[17] M. N. Legenkiy and A. Y. Butrym, "Pulse signals in open circular dielectric waveguide," *Progress In Electromagnetics Research*, vol. 22, pp. 9–17, 2011.

[18] T. L. Jensen, M. L. Jakobsen, J. Østergaard, J. K. Nielsen, C. Byskov, P. Bæk, and S. H. Jensen, "Online estimation of wind turbine blade deflection with UWB signals," in *2015 23rd European Signal Processing Conference (EUSIPCO)*. IEEE, 2015, pp. 1182–1186.

[19] [Online]. Available: www.speag.com/products/dak/dak-dielectric-probe-systems/dak3-5tl-p-200mhz-20ghz/

[20] J.-P. Berenger, "Long range propagation of lightning pulses using the FDTD method," *IEEE Trans. Electromagn. Compat.*, vol. 47, no. 4, pp. 1008–1011, 2005.

[21] O. Franek, S. Zhang, K. Olesen, P. C. F. Eggers, C. Byskov, and G. F. Pedersen, "Application of numerical dispersion compensation of the Yee-FDTD algorithm on elongated domains," in *Electromagnetics in Advanced Applications (ICEAA), 2017 International Conference on*. IEEE, 2017, pp. 1243–1246.

[22] O. Franek and G. F. Pedersen, "Spherical horn array for wideband propagation measurements," *IEEE Trans. Antennas Propag.*, vol. 59, no. 7, pp. 2654–2660, 2011.

[23] [Online]. Available: www.keysight.com/en/pdx-x201914-pn-N5231A/pna-l-microwave-network-analyzer-135-ghz

Ondřej Franek (S'02–M'05) received the Ing. (M.Sc.E.E. Hons.) and Ph.D. degrees in electronics and communication technology from Brno University of Technology, Brno, Czech Republic, in 2001 and 2006, respectively. He is currently an Associate Research Professor with the Department of Electronic Systems, Aalborg University, Aalborg, Denmark, where he is a member of the Antennas, Propagation and Millimeter-wave Systems Section. His research interests include electromagnetic theory and computational electromagnetics with a focus on fast and efficient numerical methods, especially the finite-difference time-domain method. He has developed the in-house fully scalable parallel FDTD code that has been used in research at Aalborg University to solve electrically large problems related to antennas, radiowave propagation and electromagnetic compatibility. During his career he has been involved in several research projects on various aspects of electromagnetics, particularly biological effects of nonionizing electromagnetic radiation, indoor radiowave propagation, electromagnetic compatibility, MIMO OTA testing and UWB propagation.

Dr. Franek was a recipient of the Seventh Annual Siemens Award for outstanding scientific publication.

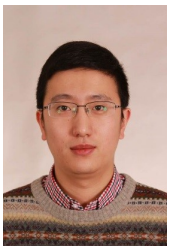

Shuai Zhang received the B.E. degree from the University of Electronic Science and Technology of China, Chengdu, China, in 2007 and the Ph.D. degree in electromagnetic engineering from the Royal Institute of Technology (KTH), Stockholm, Sweden, in 2013. After his Ph.D. studies, he was a Research Fellow at KTH. In April 2014, he joined Aalborg University, Denmark, where he currently works as Associate Professor. In 2010 and 2011, he was a Visiting Researcher at Lund University, Sweden and at Sony Mobile Communications AB, Sweden, respectively. He was also an external antenna specialist at Bang & Olufsen, Denmark from 2016–2017. He has coauthored over 40 articles in well-reputed international journals and over 14 (US or WO) patents. His research interests include: mobile terminal mmwave antennas, biological effects, CubeSat antennas, UWB wind turbine blade deflection sensing, MIMO antenna systems, and RFID antennas.

Kim Olesen received his M.Sc.E.E. degree in 1988 from Aalborg University, Denmark. He is currently employed at Aalborg University, as Head of the laboratories with special responsibilities for the radio and antenna laboratory. He has been involved in antenna measurements, channel sounding, massive MIMO and mm-wave measurements, as well as over-the-air testing of active wireless devices and radio on the fiber.

Patrick C. F. Eggers was born in Stockholm, Sweden 1957. He received the M.Sc.E.E. and Ph.D. degree from Aalborg University, Aalborg, Denmark, in 1984 and 2003 respectively.

He has been employed at Aalborg University since 1984, mainly as a full-time researcher within wireless radio communications. His current position is Associate Professor within the Antennas, Propagation and Millimetre-wave Systems section at Aalborg University. He has been an active participant in a sequence of wireless communications related COST actions, starting from COST207. He worked in Wellington, New Zealand, from 1988 to 1989 for Telecom New Zealand, on multi diffraction path-loss modelling. He has been responsible for the planning and analysis of propagation work in domestic and EU projects like TSUNAMI and CELLO.

He is the initiator of the established English-taught international M.Sc.E.E. course at Aalborg University, specializing in wireless communication. His main interests lay in the field of propagation and wireless communications. His current focus is on angular propagation characteristics related to multi-antenna system operation (Massive MIMO) and statistical channel modelling for example for ultra-reliable communications - as well as channel characterisation in harsh environments relevant for the TETRA system or sensor based systems with nearfield disturbances.

Claus Byskov was born in 1962. He received the M.Sc.E.E. degree from Aalborg University, Aalborg, Denmark, in 1986, and the M.B.A. degree from the Aarhus School of Business, Aarhus, Denmark, in 2001. He is currently with LM Wind Power, Lunderskov, Denmark, and leading new technology development initiatives for making intelligent blades. His current research interests include collaboration between research institutes and corporate business, development and commercialization of new technology, and lean startup inspired management.

Gert Frølund Pedersen was born in 1965. He received the B.Sc. and E.E. (Hons.) degrees in electrical engineering from the College of Technology in Dublin, Dublin Institute of Technology, Dublin, Ireland, in 1991, and the M.Sc.E.E. and Ph.D. degrees from Aalborg University, Aalborg, Denmark, in 1993 and 2003, respectively. Since 1993, he has been with Aalborg University where he is a Full Professor heading the Antennas, Propagation and Millimeter-wave Systems Lab with 25 researchers. He is also the Head of the Doctoral School on wireless communication with some 40 Ph.D. students enrolled. His research interests include radio communication for mobile terminals, especially small antennas, diversity systems, propagation, and biological effects. He has published more than 500 peer-reviewed papers, 6 books, 12 book chapters and holds over 50 patents. He has also worked as a Consultant for developments of more than 100 antennas for mobile terminals including the first internal antenna for mobile phones in 1994 with lowest SAR, first internal triple-band antenna in 1998 with low SAR and high TRP and TIS, and lately various multiantenna systems rated as the most efficient on the market. He has worked most of the time with joint university and industry projects and have received more than 21 M$ in direct research funding. He is currently the Project Leader of the RANGE project with a total budget of over 8 M$ investigating high performance centimetre/millimetre-wave antennas for 5G mobile phones. He has been one of the pioneers in establishing over-the-air measurement systems. The measurement technique is now well established for mobile terminals with single antennas and he was chairing the various COST groups with liaison to 3GPP and CTIA for over-the-air test of MIMO terminals. He is currently involved in MIMO OTA measurement.